Journal of Engineering Science and Technology
Vol. 8, No. 4 (2013) 416 - 427

MONOTONIC AND CYCLIC LOADING SIMULATION OF STRUCTURAL STEELWORK BEAM TO COLUMN BOLTED CONNECTIONS WITH CASTELLATED BEAM

SAEID ZAHEDI VAHID*, S. A. OSMAN, A. R. KHALIM

Department of Civil & Structural Engineering, Faculty of Engineering & Built Environment, Universiti Kebangsaan Malaysia 43600 Bangi Selangor DE, Malaysia
*Corresponding Author: sdzahedi@yahoo.com

Abstract

Recently steel extended end plate connections are commonly used in rigid steel frame due to its good ductility and ability for energy dissipation. This connection system is recommended to be widely used in special moment-resisting frame subjected to vertical monotonic and cyclic loads. However improper design of beam to column connection can leads to collapses and fatalities. Therefore extensive study of beam to column connection design must be carried out, particularly when the connection is exposed to cyclic loadings. This paper presents a Finite Element Analysis (FEA) approach as an alternative method in studying the behavior of such connections. The performance of castellated beam-column end plate connections up to failure was investigated subjected to monotonic and cyclic loading in vertical and horizontal direction. The study was carried out through a finite element analysis using the multi-purpose software package LUSAS. The effect of arranging the geometry and location of openings were also been investigated.

Keywords: Castellated beam, Cyclic loading, Finite element analysis, Earthquake.

1. Introduction

The behavior of steel moment-resisting frames (MR) is greatly affected by the properties of the beam-to-column connections, especially in seismic zones. The traditional view is to use rigid and full strength beam-to-column connections in the steel MR frames in seismic areas. However, after the North-ridge earthquake–California-1994, bolted connections which are generally semi-rigid and partially resistant have been extensively studied. A considerable number of literatures have been published on the seismic behavior of the extended end-plate connections which are the common type of bolted connections. Past research showed that steel

connections are ductile and has good ability to dissipate energy safely when subjected to either seismic or cyclic loading. The ductility of the connection depends on the thickness of the end plate and the diameter of bolts. Therefore, it is possible to design a connection that possesses sufficient ductility by selecting relatively thinner end plate with large diameters bolts.

Many researchers have conducted experimental and theoretical programs to observe the behavior of extended end-plate connections under monotonic, cyclic, and seismic loads. Butterworth [1] used a full scale testing in order to investigate extended end-plate beam-to-column connections. It was found that the higher loading on the connection, the greater distribution of stress into the web beam. Theoretically, Hasan et al. [2] presented a model of an unstiffened flush end plate connection. In this model, welds, bolt heads, and column fillets were not included, where their contributions to moment-rotation characteristics were insignificant. Machaly et al. [3] conducted a parametric analysis of steel, fully welded beam to column connection using the T-Stiffener to determine the effect of connection, geometric parameters on moment and stress distribution based on simple mathematical models and finite element results. They proposed a set of design equations that describe the T-stiffener flange and weld thickness, flange and web weld sizes and portion of applied moment supported by the T-stiffener flange and web welds.

Sherbourne and Bahaari [4] developed a methodology to evaluate analytically the moment rotation relationships for the steel bolted end-plate connections using finite element software, it was concluded that, at the ultimate load, the preloading on the bolts does not affect both, the prying action and the distribution of the forces in the beam flange. The bolt size, however, has significant effect on the prying action. Sherbourne and Bahaari [4] investigated the four-bolt unstiffened extended end-plate connections using finite element software package, ANSYS. They conducted two dimensional analysis using plane-stress elements. Later, they established a three dimensional model. In their new model, plate elements were used to model the end- plate, beam, and column; bolt head and nut were modeled using eight-node isoperimetric solid elements; each bolt shank was modeled using six bar elements; and interface elements were used to model the interaction between column flange and end-plate. In both models, bolt pretension was not considered.

Krishnamurthy [5] mentioned that there was a major shortcoming with regard to the previous Sherbourne and Bahaari [4] 3D model. He mentioned that plate or shell elements could not accept or develop ‘‘through-thickness’’ effects perpendicular to the neutral face of the plate. Furthermore, the ‘‘through-thickness’’ effect in the plates could be very dominant especially when the bolts were pre-tensioned. Sherbourne and Bahaari [4] extended their research on end-plate connections using the same 3D model as they had previously used except that pre-tensioned bolts were considered instead of hand-tightened bolts. Distribution of contact forces and stress contours in end-plate was presented graphically.

Mays [6] examined the seismic response of previously conceived end-plate configurations and proposed a design procedure for a new end-plate configuration called 16-bolt extended stiffened (16ES) that can satisfy the current code requirements. The results of this computational study were validated by a direct comparison with numerous experimental tests performed at Virginia Tech.

Zhou [7] developed a three-dimensional finite element model to simulate the behavior of eight-bolt stiffened beam to column end-plate connections. Different

approaches were used to simulate the bolt-pretension. The three-parameter power model was chosen to represent the moment-rotation behavior of the connections.

Castellated beams are I-beams or girders with notches cut from the center member. The notches, whether they are square as in a castle or octagonal or any other shape, are to reduce the weight of the beam without greatly reducing its strength. This results in a beam with a higher strength-to-weight ratio. In this study, a castellated beam-to-column connection with hexagonal cell was modeled. Figure 1 shows the standardized castellated beam where the variables are cell diameter and cell spacing. Through this simulation study, the behaviors of beam-to- column connections were investigated when subjected to both monotonic and cyclic loading in both vertical and horizontal direction.

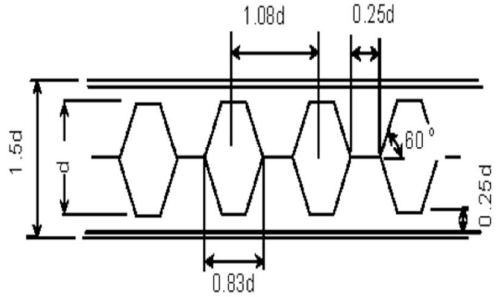

Fig. 1. Standardized Castellated Beam [8].

2. Non-Linear Finite Element Analysis

2.1. Description of the models

Five models of beam- to- column connections were selected in this study, in which the first model was a control model (model 1,) with plane beam-column connection carried out by Butterworth [1]. The other models of C1, C2, C3, and C4 were the castellated beam-column connection with hexagonal cells. The parametric studies on different variables such as size of cells, spacing and number of cells were also been carried out. Table 1 shows the details description of each model.

Each model basically consisted with the same size of beam 356x171x51UB and 1000 mm in length. Details of connections for all models are shown in Fig. 2. All models were simulated using finite element package LUSAS. Three dimensional of non-linear analysis were carried out for all models.

Table 1. Description of the Models.

Model	Cell Diameter	Cell Spacing	Cell Number
Experimental Model	-	-	-
Model 1	-	-	-
C1	200 mm	50 mm	4
C2	200 mm	100 mm	3
C3	300 mm	25 mm	3
C4	300 mm	100 mm	3

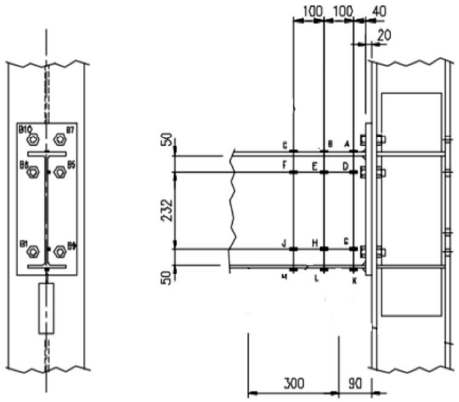

Fig. 2. Details of Connections [1].

2.2. Material properties

Table 2 shows the details description of steel materials used for beam, column and end plate in each model, whilst the high strength steel material was used for the bolts with initial yield stress of 600 N/mm^2. Figure 3 shows the constitutive stress-strain curve for bolts, beam, column and end-plate.

Table 2. Steel Materials

Materials properties	Steel
Elastic Modulus Young	2.09×10^5 N/mm^2
Poisson Ratio	0.3
Plastic	
Initial uniaxial yield stress	406 N/mm^2
Hardening gradient	2121 N/mm^2
Plastic strain	1

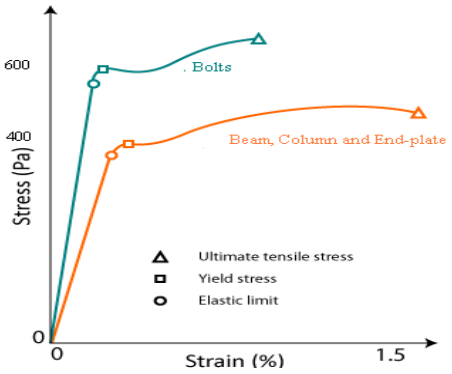

Fig. 3. Constitutive Stress-strain Curve for Bolts, Beam, Column and End-plate.

2.3. Simulation analysis

Simulations for all models were carried out in monotonic and cyclic loading analysis. Comparison of the simulation results with the laboratory test results for model 1 was also carried out to ensure the accuracy of simulation procedure. The finite element analysis results were compared to examine the validity and predictability of the developed FE model. The 50 mm x 50 mm mesh size was chosen for all models. The chosen mesh size was obtained based on the results of convergence studies on this connection system.

2.4. Element types

Figure 4 shows the five types of element used for all models. HX8M elements are three dimensional solid hexahedral elements comprising 8 nodes each with 3 degrees of freedom. These elements were used to model the beam flanges, end plate and connecting column flange. QTS4 and TTS3 elements are three dimensional flat facet thick shell elements comprising either 3 or 4 nodes each with 5 degrees of freedom and are used to model the beam and column webs, beam closing plate, column back flange and stiffeners. JNT4 elements are non-linear contact gap joint elements and are used to model the interface between the end plate and the column flange. The bolts were modeled using BRS2 elements for the bolt shank and HX8M elements for the head and nut. Typical mesh generated for all elements with supports and loading applied to the first model in LUSAS is shown in Fig. 5. Whilst mesh generated for the second model castellated beam-column connection is shown in Fig. 6.

Fig. 4. FEA Elements.

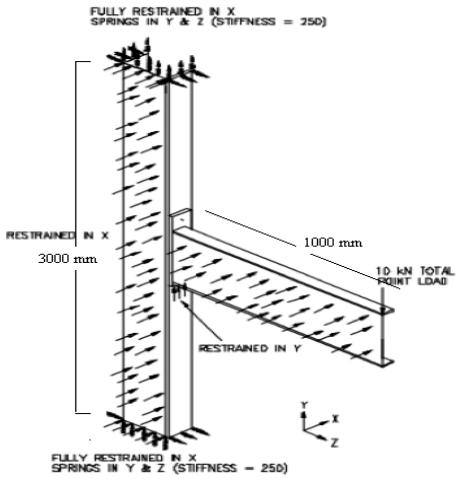

Fig. 5. FEA Supports and Loading [1].

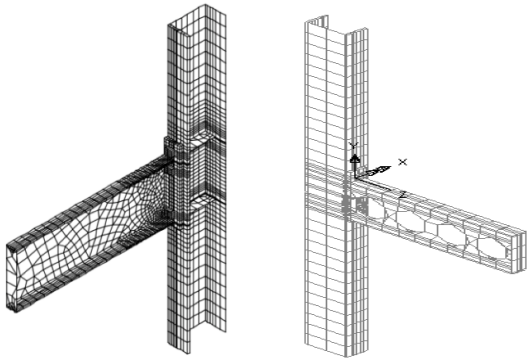

Fig. 6. Mesh Discretisation.

2.5. Boundary conditions

Based on the experimental setup by Butterworth [1], the boundary conditions were as follows where displacements in the X, Y and Z directions were restrained at the top and bottom of the half column. Displacements in the X direction were restrained along all surfaces on the center line of the model. Due to convergence problem found by the model when beam end plate had no support restraint in Y direction, therefore support has to be added to the underside of the end plate. The column to end plate interface was modeled using JNT4 joint elements with a contact spring stiffness K of 1 x 10^9 N/mm^2.The monotonic loading was applied via a 10 kN point load on the cantilever end. The load was then factored in the control file to achieve the required range of connection bending moments. The cyclic loading history used is illustrated in Fig. 7. The deformation parameter used to control the loading history is the inter story drift angle, defined as inter story displacement divided by story height. In the experimental study if the vertical beam deflection is controlled, the drift angle is defined as the beam deflection divided by the beam span (to the column centerline) whereas if the horizontal column deflection is controlled, the drift angle is defined as the column deflection divided by the column height. Whilst in this study, both of the vertical beam and horizontal column deflections were controlled.

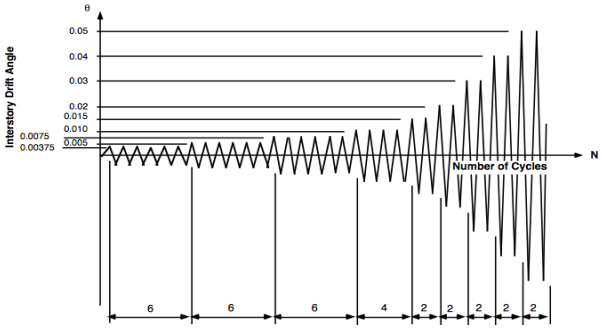

Fig. 7. Standard Cyclic Loading.

3. Results and Discussion

3.1. Verification of material modeling

The comparison of the LUSAS simulation results for model 1 with the laboratory test carried out by Butterorth [1] showed that the load-displacement curves were comparable. It shows that the maximum load carrying capacity from FE modeling is 300 kN and whilst from Experimental [1] is 290 kN, as shown in Fig. 8. According to the results, due to vertical monotonic loading as shown in Fig. 9, the ultimate load of the castellated model C3 is less than those of the other connection models (58 kN). The castellated model C1 shows to have the highest connection moment than those of the other connection models. (270 kN). It can be seen that spacing has significant effect on the ultimate capacity in model C3 and C4 respectively with the spacing of 25 mm and 100 mm whilst model C4 showed increase in the loading capacity (150 kN). According to the results, due to horizontal monotonic loading as shown in Fig. 10, the load capacity drop drastically due to the longitudinal shear transfer mechanism for all castellated models compare to solid model 1 (60 kN to 110 kN). It can be seen after a sharp drop in loading capacity that spacing, cell number and size of cells has no significant effect on the ultimate capacity among all the castellated models because the exact finished depth was fixed.

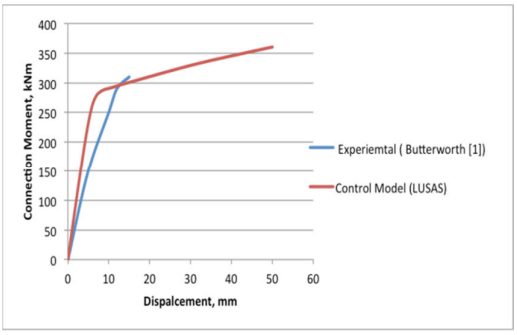

Fig. 8. Load-Displacement Curve for Model 1 and Model 2 under Monotonic Loading.

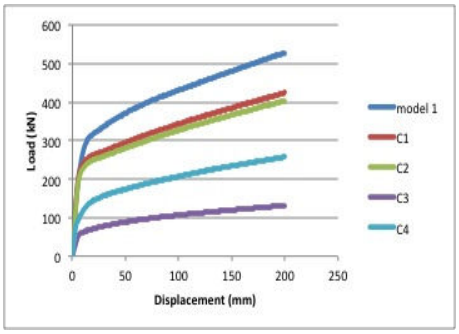

Fig. 9. Load-Displacement Curve for Castellated Models under Vertical Monotonic Loading.

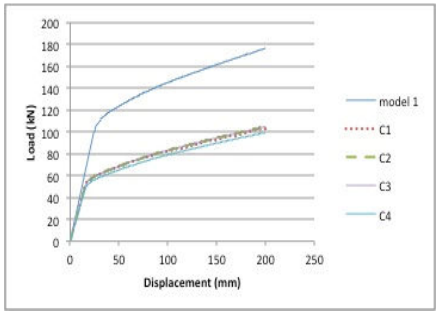

Fig. 10. Load-Displacement Curve for Castellated Models under Horizontal Monotonic Loading.

Figures 11-14 show the comparison behavior of the two types of connections subjected to cyclic loading in terms of load vs. displacement. It can be seen that model 1 has a higher strength in both vertical and horizontal loading. Model C2 exhibits a relatively higher yielding load of approximately 250 kN with yield displacement of 42 mm corresponding displacement in vertical loading. Whilst for horizontal loading, the yielding load was decreased with same value around 75 kN for all the castellated models. On the other hand, in vertical loading model C3 and C4 demonstrates lower yielding load for only 80 kN.

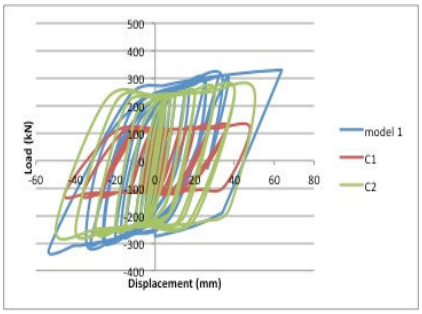

Fig. 11. Hysteresis Loops for Models C1 and C2 under Vertical Cyclic Loading.

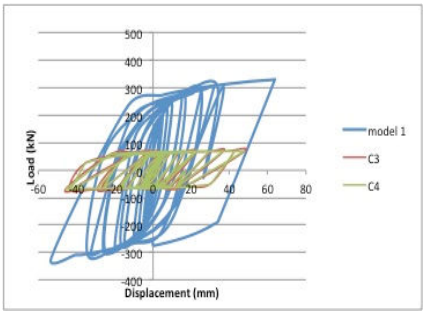

Fig. 12. Hysteresis Loops for Models C3 and C4 under Vertical Cyclic Loading.

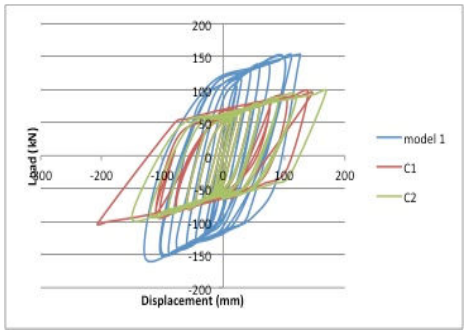

Fig. 13. Hysteresis Loops for Models C1 and C2 under Horizontal Cyclic Loading.

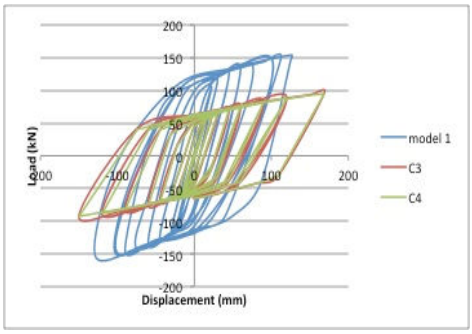

Fig. 14. Hysteresis Loops for Models C3 and C4 under Horizontal Cyclic Loading.

The amount of energy absorbed during earthquake can be measured through the equivalent viscous damping of the system. The percentage of equivalent damping can be calculated by dividing the area under the hysteresis loop (load versus displacement) over average area under maximum strength in forward and reverse loading directions. The equation used to calculate the equivalent viscous damping for the connection can be expressed as given below [6]:

$$\varepsilon = \frac{D}{2P\pi} \times 100 \quad (1)$$

where ε is the equivalent viscous damping ratio in percent, D is the hysteretic damping (dissipated energy during one cycle), and P is the potential energy for the same cycle.

Figure 15 shows the percentage values equivalent viscous damping for three different types of connection which denoted as model 1, C2 and C4. Figure 16 shows the dissipated hysteretic energy up to certain drifts for model 1, C1 and C3 under horizontal cyclic loading. Model 1 absorbed a lot of energy as compared to C3 and C1. The first cycle of model 1 has the greatest percentage equivalent viscous damping which is 14.78% as compared to the second cycle (12%). In earthquake, the first strike will destroy most of the buildings, infrastructures and

lifeline as compared aftershock. Normally, the first strike of earthquake released a lot of energy and this energy will destroy and damage the buildings and infrastructures as compared to aftershock. The area under the load-displacement curve is equal to the energy dissipated by the connection. According to equivalent viscous damping versus drift for models 1, C2 and C4 under vertical cyclic loading, model 1 absorbed a lot of energy as compared to model C2 and model C4 respectively, which means that model 1 suffered a lot of damage, followed by C2 and finally C4.

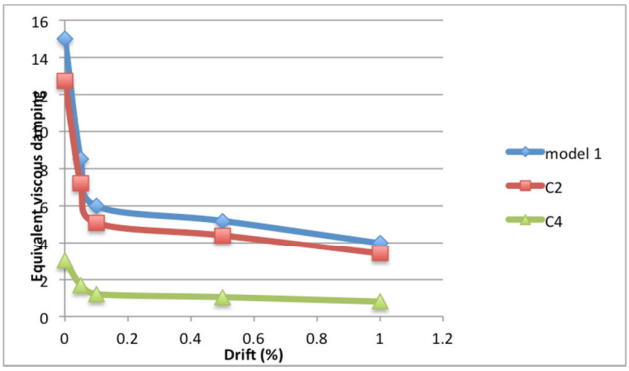

Fig. 15. Equivalent Viscous Damping vs. Drift for Models 1, C2 and C4 under Vertical Cyclic Loading.

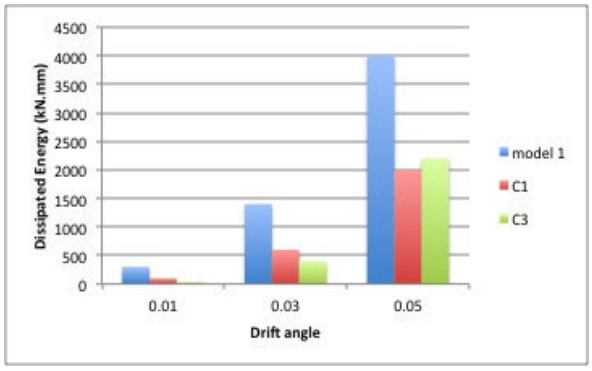

Fig. 16. Dissipated Hysteretic Energy up to certain Drifts for Models 1, C1 and C3 under Horizontal Cyclic Loading.

Figures 17 and 18 show the deflected shape of the models and the interface gap opening. The castellated connection model had small gap between column and beam interface compared to the solid model (model 1). It shows that solid model is more stable in large displacement and model failed in smaller displacement due to instability of frame which means in the solid model, beam and column failed before connection joint failed whereas the castellated model failure caused by connection joint failure.

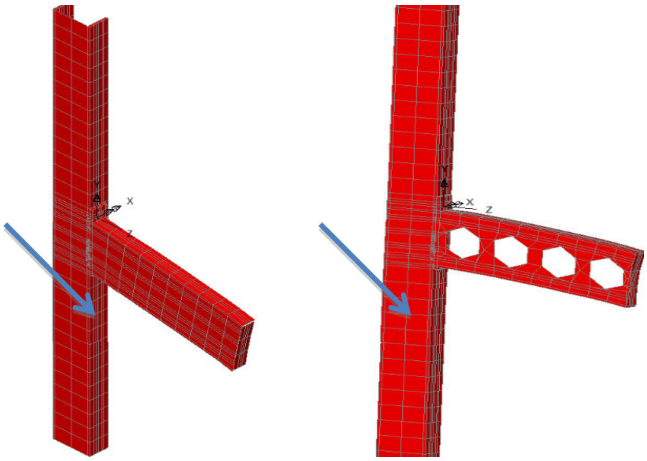

(a) Control Model **(b) Cellular Models**

Fig. 17. Deflected Shape and Interface Gap Opening due to Vertical Loading (Exaggerated Scale).

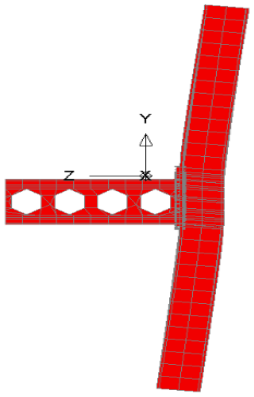

Fig. 18. Deflected Shape and Interface Gap Opening due to Horizontal Loading.

4. Conclusions

In this paper, a three dimensional finite element model using the computer package LUSAS is developed for structural behavior studies of steel connection systems under cyclic loading. Two models of beam- to- column connections were simulated to failure. Through series of simulation modeling, the following conclusions are drawn:

- The joints should have adequate strength and stiffness to resist the internal forces induced by the framing members and external force like earthquake and wind loadings.

- Based on the hysteresis curve, it shows that the performance of end plate bolted connection model simulated by LUSAS is comparable to experimental results and simulation analysis by other researchers.
- The castellated model behaved softer therefore dissipated more energy than normal plane beam to column connection.

Acknowledgments

The authors are grateful for the financial support given by The Ministry of Higher Education Malaysia through grant ERGS/1/2012/TK03/UKM/02/4.

References

1. Butterworth, J. (1997). *Finite element analysis of structural steelwork beam to column bolted connections*. Constructional Research Unit, School of Science & Technology, University of Teesside.
2. Hasan, R.; Kishi, N.; Chen, W.F.; and Komuro, M. (1997). Evaluation of rigidity of extended end-plate connections. *Journal of Structural Engineering*, 123(12), 1595-1602.
3. Machaly, E.B.; Safar, S.S.; and Youssef, M.A. (2004). Parametric analysis of welded beam-to-column connections with T-stiffener. *Journal of Engineering and Applied Sciences*, 51(1), 47-66.
4. Sherbourne, A.N.; and Bahaari, M.R. (1991). 3D simulation of end-plate bolted connections. *Journal of Structural Engineering,* 120(11), 3122-3136.
5. Krishnamurthy, N. (1996). Discussion on 3D simulation of end-plate bolted connections. *Journal of Structural Engineering*, 122(6), 713-714.
6. Mays, T.W. (2000). *Application of the finite element method to the seismic design and analysis of large moment end-plate connections*. Ph.D. thesis, Virginia Polytechnic Institute and State University, USA.
7. Zhou, F. (2005). *Model-based simulation of steel frames with endplate connections*. Ph.D. Thesis, the Division of Research and Advanced Studies, the University of Cincinnati, Ohio, USA.
8. Soltani, M.R.; Bouchaïr, A.; and Mimoune, M. (2012). Nonlinear FE analysis of the ultimate behavior of steel castellated beams. *Journal of Constructional Steel Research*, 70, 101-114.